PHYSICAL REVIEW E **69**, 055401(R) (2004)

Bernstein–Greene–Kruskal solitary waves in three-dimensional magnetized plasma

Li-Jen Chen,[1] David J. Thouless,[2] and Jian-Ming Tang[1]
[1]*Department of Physics and Astronomy, University of Iowa, Iowa City, Iowa 52242-1479, USA*
[2]*Department of Physics, University of Washington, Seattle, Washington 98195-1560, USA*
(Received 5 March 2003; published 25 May 2004)

We study the width-amplitude relation for three-dimensional Bernstein-Greene-Kruskal (BGK) electrostatic solitary waves in magnetized plasmas, taking into account the dynamics of both electrons and ions. We obtain two coupled inequalities that constrain the amplitude and the widths parallel and perpendicular to the magnetic field for a Gaussian potential, and demonstrate how the solution space is further constrained by the finite temperature ratio between electrons and ions. The description is valid for both the electron and ion mode solitary waves. Our results provide a quantitative basis for understanding the ubiquity of BGK waves in widely different classes of collisionless plasmas.

DOI: 10.1103/PhysRevE.69.055401 PACS number(s): 52.35.Sb, 52.35.Mw, 52.35.Fp

Coherent structures with nonuniform charge densities are ubiquitous in plasma systems. Laboratory experiments have shown that such structures can be generated by applying voltage pulses [1,2], voltage jumps [3], intense laser [4], or plasma beam injections [5]. Increasing numbers of space-borne observations have revealed frequent appearance of electrostatic solitary structures in space plasmas (Refs. [6,7], and references therein), including regions where magnetic reconnection occurs [8,9]. Solitary waves can efficiently transport energy, momentum, and charge, and are one of the building blocks in a deterministic description of turbulence [10,11]. The study of their allowed parameter space is crucial in establishing their relevance to real systems. Most solitary waves, such as those for shallow water (Korteweg–de Vries solitons) and those that describe crystal dislocations (sine–Gordon solitons), have a strict one-to-one mapping between their widths, amplitudes, and velocities [12]. On the other hand, in collisionless plasmas, the Bernstein-Greene-Kruskal (BGK) solitary waves [13] that exhibit vortex structures in phase space are less tightly constrained. The only constraint that delineates the allowed parameter space is the non-negativity of the trapped particle phase-space density [13], and the macroscopic manifestation of this constraint is the inequality relation between the width and amplitude of a solitary potential. The one-dimensional (1D) width-amplitude relations have been studied for various potentials and ambient plasma distributions [14–17]. However, the focus has been exclusively on whether the width of the solitary potential should increase [14,17] or decrease [15,16] with increasing potential amplitudes. The inequality aspect and its possible impact have not been discussed.

Little is known about the width-amplitude relations of BGK solitary waves in three dimensions (3D), and how the relations are modified when the dynamics of both ions and electrons are included. The few studies on the relations in 3D are for the electron mode solitary waves without including ion dynamics [18–21]. In these studies, applications to space observations of electrostatic solitary waves have been extensively discussed; however, they lack fully self-consistent solutions that constrain the widths and amplitudes for the specific models considered therein. In this article, we derive inequality width-amplitude relations for 3D BGK solitary waves based on fully self-consistent solutions, and we incorporate the dynamics of both electrons and ions. The description is valid for the electron mode as well as the ion mode. We find two coupled inequalities that constrain the amplitude and the widths parallel and perpendicular to the magnetic field, and the solution space is further constrained when the dynamics of the second species is added. The inequality width-amplitude relations dictate a continuous range of admissible sizes and amplitudes for these waves, and support their ubiquitous presence in widely different classes of collisionless plasmas. Our exact results in the strong-magnetic-field limit provide important guidance for future simulation studies on 3D BGK solitary waves in finite fields.

To construct exact nonlinear solutions that are localized in 3D, we use the BGK approach that was formulated for 1D nonlinear Vlasov-Poisson equations [13], but extend the Poisson equation to 3D. We construct azimuthally symmetric solutions in the limit of infinite magnetic field. The criteria for neglecting effects of nonzero cyclotron radius will be discussed later. One key step in the BGK approach is to separate particles that are trapped in the potential and those that are passing. We prescribe the potential form and the passing particle distribution, solve for the trapped particle distribution, and derive the physical parameter range. This approach is much easier than prescribing the passing and trapped particle distributions to solve for the potential [15,16], and so allows us to explore the solution space in much greater depth.

We consider two species of charge carriers (electrons and one type of ions), each with charge q_s, mass m_s, and ambient thermal energy T_s. The background magnetic field $\mathbf{B}$ is along the $\hat{z}$ direction. In the strong field limit, particles move only along $\mathbf{B}$ with velocity v, and the distribution function f_s satisfies the following Vlasov equation:

$$v\frac{\partial f_s(\mathbf{r},v)}{\partial z} - \frac{q_s}{m_s}\frac{\partial \Phi(\mathbf{r})}{\partial z}\frac{\partial f_s(\mathbf{r},v)}{\partial v} = 0, \tag{1}$$

where $\Phi(\mathbf{r})$ is the electrostatic potential, and we choose the boundary condition $\Phi(\infty)=0$ for our solitary wave study. It can be shown easily by chain rules that any $f(\mathbf{r}_\perp, w)$ is a

solution to Eq. (1), since its dependence on z and v is only through the particle energy $w=m_s v^2/2+q_s\Phi(\mathbf{r})$. Such distribution functions and the potential are further constrained by the Poisson equation

$$-\nabla^2\Phi(\mathbf{r})=\sum_{s=1}^{2}\int_{q_s\Phi(\mathbf{r})}^{\infty}dw\frac{4\pi n_s q_s f_s(\mathbf{r}_\perp,w)}{\sqrt{2m_s[w-q_s\Phi(\mathbf{r})]}},\qquad(2)$$

where the velocity space integral has been converted to energy space integral, and $f_s(\mathbf{r}_\perp,w)$ is normalized so that n_s is the particle density in the unperturbed region where charge neutrality gives $\Sigma_s\, n_s q_s=0$. Species 1 is defined to be the one which involves trapping $(\min[q_1\Phi(\mathbf{r})]<0)$, and species 2 does not. The distribution function f_1 is further divided into passing $(w>0)$ and trapped $(w<0)$ components, labeled as f_p and f_{tr}, respectively. The second term in Eq. (1) is nonlinear, as Φ is a functional of the particle distributions and vice versa. In physical terms, the system is nonlinear because plasma particles collectively determine the mean-field potential, and the potential in turn determines how particles distribute themselves. It is the presence of this nonlinear term that admits solitary wave solutions which exhibit localized structures in potentials and distribution functions.

Equation (1) can be thought of as a set of 1D Vlasov equations in the $\hat{z}$ direction for given $\mathbf{r}_\perp$. These parallel Vlasov equations are coupled by the perpendicular profile of the potential Φ through Eq. (2). If Φ is known, Eq. (2) reduces to a set of 1D integral equations parametrized by $\mathbf{r}_\perp$. For given f_2 and f_p, the trapped distribution f_{tr} can be found by solving these integral equations. The requirement for the solutions to be physical is that the trapped distribution f_{tr} so determined should be non-negative. This leads to a self-consistent constraint on the form of the potential specified at the beginning. It turns out that neither the potential forms nor the passing distributions are tightly constrained. One can prescribe different localized potential functions or different passing particle distributions (as long as the distribution functions satisfy the Vlasov equation). As an example, the solitary potential is chosen to be an azimuthally symmetric double-Gaussian,

$$\Phi(r,z)=g\psi\exp(-z^2/2\delta_z^2-r^2/2\delta_r^2),\qquad(3)$$

where $g=-\mathrm{sign}(q_1)$ in order for Φ to trap species-1 particles, ψ is the potential amplitude and is positive, $r=|\mathbf{r}_\perp|$, δ_z and δ_r are the widths parallel and perpendicular, respectively, to $\mathbf{B}$. The distributions f_p and f_2 are chosen to be the Boltzmann type as they represent isotropic ambient plasmas that are the simplest and satisfy Eq. (1).

$$f_p(w)=\sqrt{2m_1/\pi T_1}\exp(-w/T_1),\qquad(4)$$

$$f_2(w)=\sqrt{2m_2/\pi T_2}\exp(-w/T_2).\qquad(5)$$

We note that in this choice, the distribution functions for particles with positive velocity and with negative velocity have been taken to be equal (isotropic), while in general they can be different as allowed by Eq. (1). By carrying out the integrals of f_p and f_2 in Eq. (2) and calculating the left-hand side of Eq. (2) with Φ given by Eq. (3), we obtain the trapped particle density

$$n_{tr}(\Phi)=\Phi\left[\frac{r^2}{\delta_r^2}\left(\frac{1}{\delta_r^2}-\frac{1}{\delta_z^2}\right)-\frac{2}{\delta_r^2}-\frac{1}{\delta_z^2}-\frac{2}{\delta_z^2}\ln\left(\frac{\Phi}{g\psi}\right)\right]-e^{-\Phi}[1-\mathrm{erf}(\sqrt{-\Phi})]+\exp(-t\Phi),\qquad(6)$$

where $t=q_2T_1/(q_1T_2)$. To simplify the expression, we have set the length unit to be $\lambda_D=\sqrt{T_1/4\pi n_1 q_1^2}$, energy unit T_1, and charge unit q_1 (Φ becomes strictly negative in units of T_1/q_1). We have also rewritten the expression in terms of the potential, a crucial step for solving the integral equation analytically. The first term in Eq. (6) is the total charge density calculated from the potential, the second term is the contribution from the passing particles of species 1, and the last term is the density of species 2.

Substituting Eq. (6) into Eq. (2), one is left with an integral equation for f_{tr}. We refer readers to Appendix B in Ref. [21] for the details of solving this Volterra-type integral equation, and simply write the solution for trapped electron distribution here

$$\frac{f_{tr}(r,w)}{\sqrt{2m_1}}=\frac{2\sqrt{-w}}{\pi}\left[\frac{r^2}{\delta_r^2}\left(\frac{1}{\delta_r^2}-\frac{1}{\delta_z^2}\right)-\frac{2}{\delta_r^2}+\frac{1}{\delta_z^2}-\frac{2}{\delta_z^2}\ln\frac{4w}{-\psi}\right]+\frac{e^{-w}}{\sqrt{\pi}}[1-\mathrm{erf}(\sqrt{-w})]-\frac{e^{tw}}{\sqrt{\pi}}\sqrt{t}\,\mathrm{erfi}(\sqrt{-tw}),\qquad(7)$$

where $w<0$, and $\mathrm{erfi}(z)=\mathrm{erf}(iz)/i$ is the complex error function which is a real function of its argument. Equation (7) is the first such solution in which density perturbations from both species are incorporated, and the temperature ratio is included as an explicit parameter. Its 1D limit represents a specific realization of the general solutions derived by BGK [13]. Equation (7) is also very valuable for future numerical or simulation studies of the stabilities of 3D BGK solitary waves, since one can set up such plasma distributions and see how various perturbations would affect the subsequent evolution.

Our results show that even when $T_i>T_e$ for electron-proton plasma, ion solitary waves (ion holes) can still exist. This can be seen most easily from the small-amplitude expansion of Eq. (6). The deviation of passing ion density from its ambient value is about $-\sqrt{|\Phi|}$, while the electron density deviation is $\Phi T_i/T_e$ (note that Φ is negative). As a result, there always exists a small wave amplitude, $\sqrt{|\Phi|}<T_e/T_i$, so that the net electron density is higher than the passing ion density. This condition ensures the non-negativity of trapped ion density under the constraint of the Poisson equation, which requires a negative charge core. The existence of ion hole solutions is thus guaranteed. This result sharply contrasts the previous result, which predicts that ion holes do not exist when $T_e/T_i<3.5$ [16].

For the solutions to be physical, f_{tr} has to be non-negative everywhere. This weak constraint gives rise to inequality width-amplitude relations. The main task for solving these inequalities is to find the global minimum of f_{tr}, which is at the center of the solitary potential in our case. We separate the parameter space into two distinct regions. For $\delta_r\leqslant\delta_z$, the

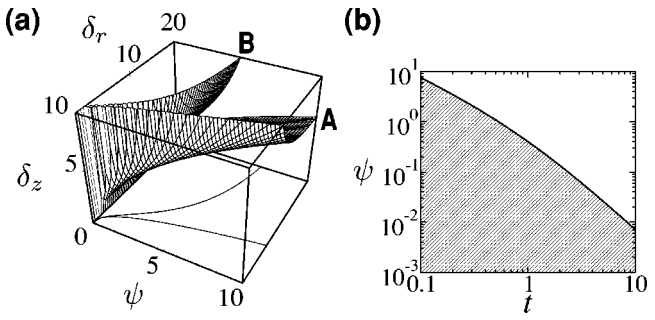

FIG. 1. Allowed parameter space for 3D BGK electron and ion solitary waves based on inequalities (8) and (9). (a) Boundaries of inequality (8) for $t=0$ (surface A) and $t=0.1$ (surface B). Points on and above the shaded surfaces represent allowed parallel size (δ_z), perpendicular size (δ_r), and potential amplitudes (ψ). The curves on the $\delta_z=0$ plane depicting inequality (9) are asymptotic projections of the two surfaces. (b) Allowed ψ for a range of $t=q_2T_1/q_1T_2$ according to inequality (9), which shows that there exists an upper bound for the potential amplitude with a given temperature ratio between electrons and ions.

first term inside the first square brackets in Eq. (7) is positive; hence, the minimum of f_{tr} for a given w is at $f_{tr}(0,w)$. Given the fact that the last two terms in Eq. (7) are positive and monotonically decreasing with $|w|$, it can be shown that the global minimum is $f_{tr}(0,-\psi)$. For $\delta_r > \delta_z$, the global minimum of f_{tr} occurs at maximum allowed r. For a given $w<0$, the maximum r at which a trapped particle with energy w can exist is the $r_{\max}$ that satisfies $-w=\Phi(r_{\max},0)$. Putting Eq. (3) into this condition, we obtain $r_{\max}^2 = -2\delta_r^2 \ln(-w/\psi)$. We then find again that the global minimum of $f_{tr}(r_{\max},w)$ is at $w=-\psi$, where $r_{\max}=0$. Therefore, in both regions, the width-amplitude relations are set by the constraint $f_{tr}(0,-\psi)\geqslant 0$.

Upon rearrangement of Eq. (7), the inequality resulting from $f_{tr}(0,-\psi)\geqslant 0$ is

$$\delta_z \geqslant \sqrt{\frac{2(4\ln 2-1)}{F_p(\psi,t)/\sqrt{\psi}-4/\delta_r^2}}, \tag{8}$$

where

$$\frac{F_p(\psi,t)}{\sqrt{\pi}} = e^{\psi}[1-\mathrm{erf}(\sqrt{\psi})] - e^{-t\psi}\sqrt{t}\,\mathrm{erfi}(\sqrt{t\psi}).$$

Since the denominator in inequality (8) has to be positive definite, additional inequalities arise

$$\delta_r^2 > 4\sqrt{\psi}/F_p(\psi,t) > 0. \tag{9}$$

Figure 1(a) plots the above inequalities for two different t values. Parameters lying on or above the shaded surface A are allowed for $t=0$, and those under the surface are forbidden. Similarly, parameters on and above the surface B are allowed for $t=0.1$. The curves on the $\delta_z=0$ plane are asymptotic projections of the shaded surfaces plotted according to the first part of inequality (9). The larger value t is, the more restricted the parameter space is. The case of $t=0$ corresponds to the limit $T_2\to\infty$, when the second species is so hot that its density is essentially unaffected by the solitary potential. This is the limit on which all previous studies on electron mode solitary waves were based.

These inequalities occur because we are free to place the global minimum of f_{tr} in a continuous range by correspondingly adjusting the amplitude and widths. A point on the shaded surface corresponds to a solution that has zero phase-space density at the center ($r=0,z=0,v=0$) of the solitary phase-space structure. The second part of inequality (9) is plotted as Fig. 1(b), which illustrates how the maximum allowed potential amplitude depends on t for a range of t that is relevant to most space and laboratory investigations. One important implication is that for a given t value, there exists a maximum allowed electric field amplitude, a consequence of the upper bound in ψ and lower bounds in δ_r and δ_z.

In the limit of $\delta_r\to\infty$, inequality (8) reduces to the width-amplitude relation for 1D BGK solitary waves. This limit yields an upper bound for δ_z that is valid for all finite δ_r at a given temperature ratio between ions and electrons. If we further set $t=0$, the resulting 1D inequality relation provides us a ground to understand the discrepancy between two previous results of whether the width should increase [14] or decrease [15] with the amplitude. Both results are contained in the inequality relation with that of Ref. [14] corresponding to the lower bounding curve, since only empty-centered distributions were studied, and that of Ref. [15] contained in the region above the curve, as the distributions only take finite values at the center of the phase-space structure.

We note that the size and the amplitude of BGK solitary waves do not have a lower cutoff within our theory. The underlying reason is that the screening of the charged core is accomplished by trapped particles which are part of the solitary structure itself. Debye screening is not involved in these self-consistent, self-sustained nonlinear objects. Their size can be well below the Debye radius as long as there are enough particles in the solitary wave to ensure the validity of the mean-field approach. Taking a Debye radius (λ_D) 100 m and a plasma density 5 cm^{-3} (typical of the low-altitude auroral ionosphere), a width of 0.01 λ_D for the solitary potential allows 5×10^6 particles in the structure, well within the applicability of the mean-field approach. Indeed, sub-Debye-scale solitary waves have been observed [6].

All the above results have been obtained in the infinite magnetic field limit. To establish the validity of these results in the finite magnetic field, we consider trapped particle trajectories inside the solitary potential. Here, we only summarize the final results, and leave the actual calculations to a future article. If the cyclotron radius is much smaller than the scale lengths over which the potential varies, the instantaneous guiding center of the particle would spiral around the infinite-field guiding center, and the solitary structure could be maintained. Both $E\times B$ drift and polarization drift are contained in our calculations. Since $E\times B$ drift is in the azimuthal direction, it is only the polarization drift that would lead to the running away of trapped particles and thus the disintegration of the solitary structure. We obtain the following criteria for neglecting the effects due to the polarization drift:

$$\sqrt{m_1\psi/q_1} \ll B\delta_z \tag{10}$$

$$\sqrt{m_1\psi/q_1} \ll B\delta_r. \tag{11}$$

Our results are consistent with those from a numerical investigation of finite-field effects [18].

The freedom to continuously adjust the global minimum of the trapped particle distribution is due to the collisionless nature of the plasma. The identities of trapped and passing particles are preserved, as the energy of a particle is conserved. Collisions destroy energy conservation of individual particles, and consequently do not allow the existence of a trapped particle state. Therefore, the kinetic solitary waves have a continuum of allowed potential heights and widths, in great distinction to fluid solitons that possess only one allowed width for a fixed amplitude. Moreover, even with the same ambient plasma distribution, different functional forms for the solitary potential are allowed. This multitude of continua of allowed potentials supports the ubiquity of BGK waves that is revealed by numerous experimental and simulation studies. Because these solitary waves have many degrees of freedom, energy, momentum, and charge are readily transferred between them, so they can make important contributions to bulk properties of the plasma such as thermal transport and electrical resistivity. As particle trapping prohibits particles from free acceleration by the applied electric field and consequently would regulate the electric current, the excitation of BGK waves may lead to finite resistivity that is required for melting the frozen-in magnetic flux and facilitate reconnection to occur in collisionless plasmas [8,9].

In summary, we have obtained trapped particle solutions for 3D BGK electron and ion solitary waves, taking into account dynamics of both species. We derived from the solutions exact inequality relations that constrain the widths and amplitudes of the solitary waves, and the temperature ratio between electrons and ions. Our results are valid for strong magnetic fields where the cyclotron radius of trapped particles is smaller than the lengths over which the solitary potential varies. We suggest that the continuum of allowed parameter space of BGK waves is responsible for their ubiquity. Our analytical solution for the trapped particle distribution provides a good foundation for future investigations on stabilities of BGK waves.

This research at the University of Iowa was supported in part by DOE Cooperative Agreement No. DE-FC02-01ER54651 and NSF ATM 03-27450, and at the University of Washington by NSF DMR-0201948.

[1] J. P. Lynov *et al.*, Phys. Scr. **20**, 328 (1979).
[2] G. Bachet *et al.*, Phys. Plasmas **8**, 3535 (2001).
[3] C. Chan *et al.*, Phys. Rev. Lett. **52**, 1782 (1984).
[4] D. S. Montgomery *et al.*, Phys. Rev. Lett. **87**, 155001 (2001).
[5] H. Klostermann and Th. Pierre, Phys. Rev. E **61**, 7034 (2000).
[6] R. E. Ergun *et al.*, Phys. Rev. Lett. **81**, 826 (1998).
[7] J. S. Pickett *et al.*, Nonlinear Processes Geophys. **10**, 3 (2003).
[8] J. F. Drake *et al.*, Science **299**, 873 (2003).
[9] H. Matsumoto *et al.*, Geophys. Res. Lett. **30**(6), 1326 (2003).
[10] P. G. Saffman, *Vortex Dynamics* (Cambridge University Press, Cambridge, 1995).
[11] *The Role of Coherent Structures in Modelling Turbulence and Mixing*, edited by J. Jimenez (Springer-Verlag, New York, 1981).
[12] P. G. Drazin, *Solitons* (Cambridge University Press, Cambridge,1983).
[13] I. B. Bernstein, J. M. Greene, and M. D. Kruskal, Phys. Rev. **108**, 546 (1957).
[14] V. A. Turikov, Phys. Scr. **30**, 73 (1984).
[15] H. Schamel, Phys. Scr. **T2/1**, 228 (1982).
[16] H. Schamel, Phys. Rep. **140**, 161 (1986).
[17] L. Muschietti *et al.*, Geophys. Res. Lett. **26**, 1093 (1999); Nonlinear Processes Geophys. **6**, 211 (1999).
[18] L. Muschietti *et al.*, Nonlinear Processes Geophys. **9**, 101 (2002).
[19] L.-J. Chen and G. K. Parks, Geophys. Res. Lett. **29**, 1331 (2002).
[20] L.-J. Chen and G. K. Parks, Nonlinear Processes Geophys. **9**, 111 (2002).
[21] L.-J. Chen, Ph.D. thesis, University of Washington, 2002. This paper can be found at http://alpha.physics.uiowa.edu/~lijen/thesis.pdf